Contract No:

This document was prepared in conjunction with work accomplished under Contract No. DE-AC09-08SR22470 with the U.S. Department of Energy (DOE) Office of Environmental Management (EM).

Disclaimer:

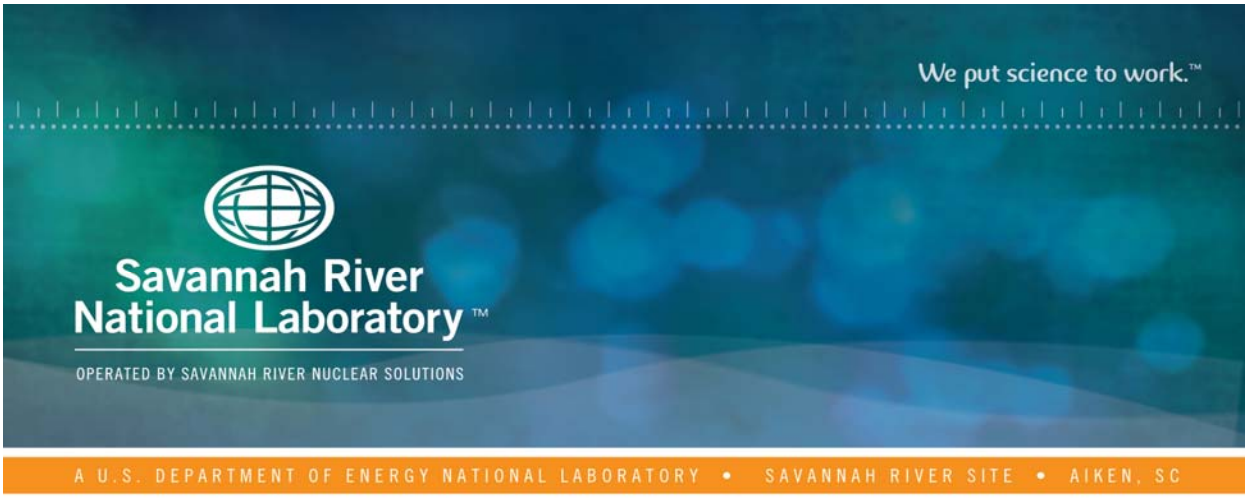

Recommendation of Ruthenium Source for Sludge Batch Flowsheet Studies

W. H. Woodham

November 2017

SRNL-STI-2017-00423, Revision 0

DISCLAIMER

Printed in the United States of America

Prepared for
U.S. Department of Energy

SRNL-STI-2017-00423
Revision 0

Keywords: *Ruthenium, DWPF, CPC*

Retention: *Permanent*

Recommendation of Ruthenium Source for Sludge Batch Flowsheet Studies

W. H. Woodham

November 2017

Prepared for the U.S. Department of Energy under contract number DE-AC09-08SR22470.

Savannah River National Laboratory™
OPERATED BY SAVANNAH RIVER NUCLEAR SOLUTIONS

REVIEWS AND APPROVALS

AUTHORS:

_____

W. H. Woodham, Process Technology Programs Date

TECHNICAL REVIEW:

_____

D. P. Lambert, Process Technology Programs, Reviewed per E7 2.60 Date

APPROVAL:

_____

F. M. Pennebaker, Chemical Processing Technologies Date

_____

D. E. Dooley, Manager Date
Chemical Processing Technologies

_____

E. J. Freed, Manager Date
DWPF/Saltstone Facility Engineering, Savannah River Remediation

_____

R. E. Edwards, Manager Date
Nuclear Safety and Engineering Integration, Savannah River Remediation

PREFACE

Included herein is a preliminary analysis of previously-generated data from sludge batches 7a, 7b, 8, and 9 sludge simulant and real-waste testing, performed to recommend a form of ruthenium for future sludge batch simulant testing under the nitric-formic flowsheet. Focus is given to reactions present in the Sludge Receipt and Adjustment Tank cycle, given that this cycle historically produces the most changes in chemical composition during Chemical Process Cell processing. Data is presented and analyzed for several runs performed under the nitric-formic flowsheet, with consideration given to effects on the production of hydrogen gas, nitrous oxide gas, consumption of formate, conversion of nitrite to nitrate, and the removal and recovery of mercury during processing.

Additionally, a brief discussion is given to the effect of ruthenium source selection under the nitric-glycolic flowsheet. An analysis of data generated from scaled demonstration testing, sludge batch 9 qualification testing, and antifoam degradation testing under the nitric-glycolic flowsheet is presented. Experimental parameters of interest under the nitric-glycolic flowsheet include N_2O production, glycolate destruction, conversion of glycolate to formate and oxalate, and the conversion of nitrite to nitrate. To date, the number of real-waste experiments that have been performed under the nitric-glycolic flowsheet is insufficient to provide a complete understanding of the effects of ruthenium source selection in simulant experiments with regard to fidelity to real-waste testing. Therefore, a determination of comparability between the two ruthenium sources as employed under the nitric-glycolic flowsheet is made based on available data in order to inform ruthenium source selection for future testing under the nitric-glycolic flowsheet.

EXECUTIVE SUMMARY

Previously published results from nine series of non-radioactive simulant and three real-waste Chemical Process Cell simulations have been reviewed and analyzed to 1) distinguish the effects of ruthenium source during simulant testing on important processing behavior, 2) determine the similarities between tests performed with each ruthenium source and tests with real waste, and 3) recommend a form of ruthenium for future Sludge Batch (SB) testing. Data were used from SB7, SB7b, SB8, and SB9 nitric-formic flowsheet testing, covering the use of ruthenium chloride ($RuCl_3$) and ruthenium nitrosyl nitrate ($Ru(NO)(NO_3)_3$). Additional data from scaled demonstration testing, SB 9 qualification testing, and antifoam degradation testing under the nitric-glycolic flowsheet were used. The following conclusions were made from the analyses described in this report:

Nitric-Formic Flowsheet

- Both $RuCl_3$- and $Ru(NO)(NO_3)_3$-containing systems are conservative in terms of H_2 production with respect to real-waste values, with $Ru(NO)(NO_3)_3$-containing systems exhibiting more conservatism than $RuCl_3$-containing systems.
- Neither catalytic simulant system is conservative in terms of N_2O production with respect to real-waste values. Of the two, $Ru(NO)(NO_3)_3$-containing systems appear to underpredict the least.
- Reaction scale appears to have an effect on N_2O production and may partially explain the tendency of 4-L simulant testing to underpredict N_2O production rates seen in 1-L real waste testing.
- $RuCl_3$-containing systems and $Ru(NO)(NO_3)_3$-containing systems behave differently in terms of formate destruction. This may be due to differences beyond those seen in H_2 production. $RuCl_3$-containing systems appear to better emulate the formate destruction seen in real waste testing.
- Nitrite-to-nitrate conversion is not significantly affected by selection of ruthenium source.
- Poor mercury balances make the affirmation of effects due to Hg_2Cl_2 formation difficult. Based on available data, ruthenium source does not appear to have any significant effect on mercury removal or recovery during Sludge Receipt and Adjustment Tank (SRAT) processing.
- Given the ratio of Ru to Hg used in SB9 testing, the presence of chloride from $RuCl_3$ added to simulant is not expected to affect the majority of mercury via formation of Hg_2Cl_2.

Nitric-Glycolic Flowsheet

- Glycolate destruction and conversion to formate are not significantly affected by the selection of ruthenium source.
- $Ru(NO)(NO_3)_3$-containing systems tend to convert more of the initially-charged nitrite and glycolate to nitrate and oxalate, respectively, than $RuCl_3$-containing systems.
- Simulant experiments conducted with $Ru(NO)(NO_3)_3$ overpredict the conversion of nitrite to nitrate. No conclusion can be drawn concerning this effect in $RuCl_3$-containing systems.
- Simulant experiments conducted with $Ru(NO)(NO_3)_3$ overpredict the conversion of glycolate to oxalate. It is uncertain if $RuCl_3$-containing systems can adequately predict the conversion of glycolate to oxalate.

In light of these conclusions, the following recommendations have been made.

1. In future SB testing under the nitric-formic flowsheet:
   - $RuCl_3$ should be used when it is more important to accurately emulate H_2 production behavior or formate destruction seen in real-waste. This will allow simulant runs to be performed conservatively, but not so much as to impractically bound any recommended acid stoichiometry window proposed during future flowsheet testing.

- $Ru(NO)(NO_3)_3$ should be used when it is more important to accurately emulate N_2O production behavior seen in real waste, or when mercury behavior is being investigated in Low Hg/High Ru sludges (Hg:Ru mass ratio of 30:1 or lower). This will guarantee that minimal Hg_2Cl_2 will be formed during processing and more closely predict the formation of N_2O, which determines the limit of nitrite-to-nitrate conversion.
- When the factors described above are negligible either ruthenium source may be used, with consideration given to availability and ease of use.

2. Further investigation should be made into the effect of scale on the production of N_2O and what effects that relationship has on the data presented in this report. In particular, effort should be made to determine the flowsheet dependence of this phenomenon and the applicability of comparison between 4-L simulant experiments to 1-L real-waste experiments.
3. Additional real-waste experiments should be performed under the nitric-glycolic flowsheet so that the chemical behavior of glycolic acid in real waste can be better defined. Since neither hydrogen formation nor formate destruction are significant processing factors in the Chemical Process Cell under the nitric-glycolic flowsheet, no recommendation can be made concerning the use of either ruthenium source in nitric-glycolic flowsheet simulant testing. Once more real-waste testing data is available, a re-evaluation should be made concerning the effect of ruthenium source on conversion of glycolate to oxalate and nitrite to nitrate. If feasible, future simulant tests under the nitric-glycolic flowsheet should include duplicate runs using both sources of ruthenium in order to provide a better understanding of the importance of source selection on processing behavior.

TABLE OF CONTENTS

LIST OF TABLES

LIST OF FIGURES

LIST OF ABBREVIATIONS

% CS	Percent Calcined Solids
% IS	Percent Insoluble Solids
% TS	Percent Total Solids
CPC	Chemical Process Cell
DWPF	Defense Waste Processing Facility
H_2	Hydrogen
Hg_2Cl_2	Mercury(I) Chloride (or calomel)
HgO	Mercury(II) Oxide
MWWT	Mercury-Water Wash Tank
KMA	Koopman Minimum Acid
N_2O	Nitrous Oxide
NM	Not Measured
$Ru(NO)(NO_3)_3$	Ruthenium(III) Nitrosyl Nitrate
$RuCl_3$	Ruthenium(III) Chloride
SB	Sludge Batch
SME	Slurry Mix Evaporator
SRAT	Sludge Receipt and Adjustment Tank
SRNL	Savannah River National Laboratory
SRS	Savannah River Site
TIC	Total Inorganic Carbon
TOF	Turnover Frequency
TON	Turnover Number

1.0 Introduction

Historically, noble metals have played an integral role in the qualification of flowsheet processing of nuclear waste in the Defense Waste Processing Facility (DWPF) at the Savannah River Site (SRS) in Aiken, SC. It has been shown that noble metals such as rhodium and ruthenium are the primary sources of catalytic formic acid dehydrogenation to form flammable H_2 during Sludge Receipt and Adjustment Tank (SRAT) and Slurry Mix Evaporator (SME) processing.[1] It is also believed that these and other noble metals (such as palladium) play a crucial role in the formation of the oxidizer N_2O.[2] In order to safely qualify each sludge batch (SB), non-radioactive sludge simulants are trimmed with noble metal salts (typically at 125% of the real-waste concentration) such that the flammable behavior of each sludge batch can be studied and mitigated.

Researchers at the Savannah River National Laboratory (SRNL) have traditionally used $RuCl_3$ during flowsheet simulant testing to emulate the effects of ruthenium during processing. Following SB8 testing, it was speculated that the use of $RuCl_3$ may have a detrimental effect on the recovery and removal of mercury during Chemical Process Cell (CPC) simulations due to the possibility of the formation of mercury(I/II) chlorides.[3] This possibility coupled with the fact that the amount of chloride added as $RuCl_3$ significantly exceeds chloride concentrations in SRS waste tanks led to the decision to use an alternative ruthenium source (ruthenium nitrosyl nitrate, $Ru(NO)(NO_3)_3$) during SB9 testing. It was noted during SB9 testing that this new ruthenium source (nitrosyl nitrate) appeared to generate more H_2 than the former ruthenium source (chloride). It was also noted that the use of this new form of ruthenium seemed to affect the generation rates of nitrogen oxides (N_2O, NO, NO_2).[3]

Following these observations, SRNL was requested to recommend a source of ruthenium for future SB testing.[4] A TTQAP was developed to outline the approach to be taken by SRNL,[5] specifying investigation into the effect of ruthenium source on the following:

- Hydrogen generation
- Nitrogen oxide generation
- Anion conversions
- Hg recovery/removal

Data from SB7, SB7b, SB8, and SB9 simulant[3,6] and real-waste[7,8] testing have been reviewed and re-analyzed to identify any effects of ruthenium source selection on processing under the nitric-formic flowsheet. Due to processing complications during testing and a lack of existing data, only SB8 and SB9 testing data was employed when considering offgas generation. Data from scaled demonstration testing, SB9 qualification testing, and antifoam degradation testing has been reviewed and analyzed to identify any effects of ruthenium source selection on processing under the nitric-glycolic flowsheet.

2.0 Historical Data

2.1 Sludge Batch 8 Testing

In 2013, Koopman reported results[6] from simulant testing performed to support the qualification of SB8. Four sludge-only runs (named D1 – D4) were performed using sludge simulant designed to closely mirror the expected composition of SB8 sludge. Each of these runs employed $RuCl_3$ as the source of ruthenium throughout testing. A real-waste demonstration of the SB8 flowsheet (named SC-14) was performed by Pareizs and Crawford in 2013[7] following the recommendations made by Koopman. Table 2-1 compares the composition of the sludge simulant used during runs D1 – D4 to that of the real waste used in SC-14. For convenience of comparison, the composition of the SB8-D simulant is also shown on an adjusted total

solids basis such that the measured percentage of total solids in the SB8-D simulant is identical to that measured in the SC-14 sludge.

Table 2-1. Physical Properties and Composition of SB8 Qualification Sludge and Sludge Simulant

Analyte	SB8-D (simulant)	SB8-D (adjusted)	SC-14 (real-waste)
% TS	18.7	22.7	22.7
% IS	10.2	12.4	13.2
% CS	14.4	17.5	17.7
Nitrate (mg/kg)	10,100	12,300	13,600
Nitrite (mg/kg)	16,100	19,500	17,700
TIC (mg/kg)	1,930	2,340	810
OH^- (mol/L)	0.856	0.88	0.79
Mn (% of CS)	8.03	8.03	8.09
Ca (% of CS)	1.41	1.41	1.44
Mg (% of CS)	0.29	0.29	0.21
Hg (% of TS)	1.25-2.14	1.25-2.14	1.96
Ru (% of TS)	0.0830	0.083	0.0398
Rh (% of TS)	0.0175	0.0175	0.0090
Pd (% of TS)	0.0034	0.0034	0.0029

It is important to note that additional testing was performed during SB8 qualification activities with alternative simulants.[9] However, these runs were not designed to mimic the conditions seen during SC-14, and therefore are not used in comparison of H_2 and N_2O generation.

2.2 Sludge Batch 9 Testing

In 2016, Smith reported results[3] of simulant testing performed to support the qualification of SB9. Eight sludge-only runs (named SB9-A1 – SB9-A8) were performed using $Ru(NO)(NO_3)_3$ and one sludge-only run (named SB9-A11) was performed using $RuCl_3$. A real-waste demonstration of the SB9 flowsheet (named SC-17) was performed by Pareizs et al in 2016[8] following the recommendations made by Smith. Table 2-2 compares the composition of the sludge simulant used during runs SB9-A1 – SB9-A11 to that of the real waste used in SC-17. For convenience of comparison, the composition of the SB9-A simulant is also shown on an adjusted total solids basis such that the measured percentage of total solids in the SB9-A simulant is identical to that measured in the SC-17 sludge.

Table 2-2. Physical Properties and Composition of SB9 Qualification Sludge and Sludge Simulant

Analyte	SB9-A (simulant)	SB9-A (adjusted)	SC-17 (real-waste)
% TS	15.3	18.7	18.7
% IS	10.6	13.0	13.0
% CS	11.74	14.4	14.7
Nitrate (mg/kg)	5,725	7000	7,320
Nitrite (mg/kg)	10,200	12,500	13,700
TIC (mg/kg)	1,619	1,980	1,600
OH^- (mol/L)	0.483	0.496	0.469
Mn (% of CS)	8.74	8.74	7.30
Ca (% of CS)	1.53	1.53	1.27
Mg (% of CS)	0.293	0.293	0.29
Hg (% of TS)	2.48	2.48	1.97
Ru (% of TS)	0.0762	0.0762	0.0563
Rh (% of TS)	0.0156	0.0156	0.0125
Pd (% of TS)	0.0037	0.0037	0.0025

2.3 Nitric-Glycolic Flowsheet Testing

The DWPF is planning to transition from the nitric-formic flowsheet to the nitric-glycolic flowsheet in the near future, thereby greatly reducing hydrogen production during nuclear waste processing. SRNL has worked to develop the nitric-glycolic flowsheet by performing over 100 simulations using non-radioactive simulants and glycolic acid (rather than formic acid). In 2016, Lambert published results from several glycolic acid flowsheet experiments designed to examine the impact of scaling on the nitric-glycolic flowsheet.[10] A subset of these experiments (named GN70-75) utilized $RuCl_3$ as the source of ruthenium, and are included here for discussion. Later in 2016, Lambert performed ten SRAT-only nitric-glycolic experiments (named NG51-59) in support of sludge batch 9 qualification using $Ru(NO)(NO_3)_3$ as the source of ruthenium.[11] In the summer of 2016, Lambert performed four abbreviated nitric-glycolic SRAT experiments focused on the formation of HMDSO.[12] Two of these runs (NG63 and NG64) used $Ru(NO)(NO_3)_3$ and $RuCl_3$, respectively (it was determined that the effect of ruthenium source selection on HMDSO was negligible within 20%). Also in 2016, Newell published results from a nitric-glycolic CPC simulation performed with real waste in support of sludge batch 9 qualification under the nitric-glycolic flowsheet.[13] The compositions of sludge used in these experiments are given below in Table 2-3.

Table 2-3. Composition of Nitric-Glycolic Flowsheet Sludges

Analyte	GN70-75 (Scaled testing)	NG51-59 (SB9 testing)	NG63,NG64 (HMDSO testing)	SB9: SC-18 (Real Waste)
%TS	17.5	15.3	17.5	17.6
%IS	11.6	10.6	11.4	12.2
%CS	12.7	11.7	12.8	13.8
Nitrate (mg/kg)	8,100	5,830	8,200	7,620
Nitrite (mg/kg)	12,400	10,300	12,800	13,700
TIC (mg/kg)	1,440	1,619	1,570	1,140
OH^- (mol/L)	0.506	0.483	0.504	0.505
Mn (% of CS)	7.4	7.8	7.8	7.12
Ca (% of CS)	1.7	1.58	1.51	1.29
Mg (% of CS)	0.3	0.283	0.28	0.286
Hg (% of TS)	2.14	2.48	2.48	2.18
Ru (% of TS)	0.0830	0.0762	0.0762	0.0566
Rh (% of TS)	0.0175	0.0156	0.0156	0.0124
Pd (% of TS)	0.0034	0.0037	0.0037	0.0025

2.4 Methods of Comparison

When analyzing the efficiency of reactions that are known to be catalytic, it is useful to estimate the lifetime and activity of the catalyst. These estimates can be performed by calculating a turnover number (TON) and turnover frequency (TOF) of the catalytic system, respectively. The TON of a catalytic system is an estimate of the average number of catalytic cycles in which a catalyst can participate before deactivation, and is typically defined as the ratio of moles of product produced to moles of catalyst employed, as shown in Equation (1):

$$TON \equiv \frac{n_{prod}}{n_{cat}} \tag{1}$$

where n_{prod} is defined as the total amount of product produced from the reaction (in moles) and n_{cat} is defined as the total amount of catalyst present in the reaction system (in moles). When considering hydrogen production via ruthenium-catalyzed formic acid dehydrogenation in nuclear waste pre-treatment simulation experiments, Equation (1) can be re-written in terms of measureable process parameters, as shown in Equation (2):

$$TON_{SRAT} = \frac{n_{H_2}}{n_{Ru}} = \frac{MW_{Ru} \cdot \int \dot{n}_{H_2} dt}{m_{sludge} \cdot \%TS \cdot \%Ru} \tag{2}$$

where TON_{SRAT} is the turnover number calculated for the SRAT cycle of the experiment in question, MW_{Ru} is the molecular weight of ruthenium (in grams per mole), $\dot{n}_{H_2}$ is the molar flow rate of hydrogen produced as a function of time (in moles per minute), n_{Ru} is the amount of ruthenium present (in moles), n_{H_2} is the amount of hydrogen produced (in moles), m_{sludge} is the mass of sludge or sludge simulant used during the experiment (in grams), $\%TS$ is the percentage of the sludge or sludge simulant comprised of solids (soluble or insoluble), and $\%Ru$ is the percentage of total solids comprised of ruthenium.

The TOF of a catalytic system is an estimate of the rate at which a catalyst is capable of completing a certain number of cycles, and is therefore a rough estimate of catalyst activity. TOF is typically defined as the ratio of the number of moles of product produced to the number of moles of catalyst, normalized by the amount of time taken to produce the specified product, as shown in Equation (3):

$$TOF \equiv \frac{n_{prod}}{n_{cat} \cdot \Delta t_{reaction}} \quad (3)$$

where $\Delta t_{reaction}$ is the duration of the reaction (in minutes). Due to the tendency of catalytic activity to change throughout a reaction, it is generally preferred to use shorter durations of incomplete reactions to compare catalyst activity. This principle can be applied to SRAT processing by using the maximum instantaneous rate of hydrogen generation, as shown in Equation (4):

$$TOF_{SRAT} = \frac{\dot{n}_{H_2}^{\max}}{n_{Ru}} \quad (4)$$

where $\dot{n}_{H_2}^{max}$ is the maximum measured rate of hydrogen generation throughout the SRAT cycle. Since it is of interest to understand the effect of ruthenium in CPC simulations, this value will be measured during the period of hydrogen generation historically associated with ruthenium activity (second peak, usually 4-9 hours after acid addition). The benefit of TON/TOF analysis in the context of noble-metal catalyzed hydrogen production in nuclear waste is that effects from multiple hydrogen-producing metals may be ignored in favor of comparing the overall efficiency of hydrogen production. Since the ratios of these metals (ruthenium, rhodium, palladium, etc.) remain relatively constant in the simulant and real-waste experiments described herein, one may assume that differences in efficiency stem from differences in ruthenium source (i.e., assume that non-ruthenium metals behave identically in simulant and real-waste testing). This assumption is especially valid in the context of sludge simulant experiments, where rhodium is invariably added to simulants as $Rh(NO_3)_3$.

2.5 Quality Assurance

The majority of data presented in this report was drawn from previously-reviewed technical reports. Requirements for performing reviews of technical reports and the extent of review are established in manual E7 2.60. SRNL documents the extent and type of review using the SRNL Technical Report Design Checklist contained in WSRC-IM-2002-00011, Rev. 2.

3.0 Results and Discussion

3.1 Effects of Ruthenium Source Selection on Hydrogen Generation

The calculated TONs and TOFs (as described in Section 2.3) for simulant and real-waste experiments for SB9 and SB8 (shaded) testing are given in Table 3-1.

Table 3-1. Catalytic Turnover Measurements for Hydrogen Production During SB8 and SB9 Flowsheet Testing Runs

Run ID	KMA (%)	Form of Ru	TON	TOF (min^{-1})
SC-17 (SB9)	120	---[a]	6.52	0.008
SB9-A2	105	$Ru(NO)(NO_3)_3$	2.69	0.003
SB9-A6	119	$Ru(NO)(NO_3)_3$	23.2	0.039
SB9-A11	119	$RuCl_3$	5.73	0.011
SB9-A8	123	$Ru(NO)(NO_3)_3$	16.9	0.032
SB9-A5	124	$Ru(NO)(NO_3)_3$	34.4	0.049
SB9-A7	124	$Ru(NO)(NO_3)_3$	3.09[b]	0.027
SB9-A3	128	$Ru(NO)(NO_3)_3$	41.2	0.052
SB9-A4	129	$Ru(NO)(NO_3)_3$	35.8	0.055
SB9-A1	144	$Ru(NO)(NO_3)_3$	80.8	0.136
SC-14 (SB8)	109	---[a]	4.49	0.004
SB8-D1	101	$RuCl_3$	1.35	0.002
SB8-D3	116	$RuCl_3$	7.55	0.014
SB8-D2	135	$RuCl_3$	12.1	0.015
SB8-D4	135	$RuCl_3$	11.6	0.016

[a]Shielded Cells runs use real-waste, which already contains ruthenium formed as a fission product.
[b]Run SB9-A7 was subject to processing issues and complications, leading to unreliable estimations of total H_2 production

It is apparent that systems employing ruthenium nitrosyl nitrate are generally more active than ruthenium chloride systems, with TOFs for $Ru(NO)(NO_3)_3$ varying between 0.003 and 0.136 min^{-1} while TOFs for $RuCl_3$ vary between 0.002 and 0.016 min^{-1}. Likewise, real-waste systems appear to be less active, with SC-14 yielding a TOF of 0.004 min^{-1} and SC-17 yielding a TOF of 0.008 min^{-1}. The same hierarchy appears to exist in catalyst lifetime, or TON, where nitrosyl nitrate systems, chloride systems, and real-waste systems exhibit TON ranges of 2.7-80.8, 1.4-12.1, and 4.5-6.5, respectively. These data suggest that ruthenium nitrosyl nitrate-containing systems are more active in the catalytic production of hydrogen than ruthenium chloride-containing systems, which in turn appear to be more active than real-waste containing systems.

A similar conclusion can be made by comparing calculated TOF and TON values to the estimated initial concentration of formate employed in each experiment, which is calculated according to Equation (5) below:

$$[HCOOH]_0 = \frac{n_{HCOOH}}{V_{supernatant}} = \frac{V_{FA} \cdot [FA] \cdot \rho_{supernatant}}{m_{sludge} \cdot (1 - \omega_{IS})} \quad (5)$$

where $[HCOOH]_0$ is an approximation of the initial concentration of formic acid on a supernatant-only basis at the beginning of a SRAT cycle (in moles per liter), V_{FA} is the volume of formic acid added (in liters), $[FA]$ is the concentration of formic acid used in the SRAT cycle (in molar), $\rho_{supernatant}$ is the density of the supernatant phase (in kilograms per liter), and ω_{IS} is the weight fraction of insoluble solids present in the sludge. It is important to note that this calculation of formic acid concentration inevitably contains systematic error due to the fact that slurry volume increases with the addition of nitric and formic acids. This error increases the calculated value of $[HCOOH]_0$ (relative to the expected value) for every run, and is slightly dependent on acid stoichiometry, sludge composition, and the percentage of added acid employed as reducing acid. Trends and relative concentrations calculated in this manner are not expected to be significantly affected by this error.

Figure 3-1 shows the calculated TOF of SB8 experiments (simulant and real-waste) plotted against their estimated initial formic acid concentrations, while Figure 3-2 shows the same data for SB9 real-waste and simulant experiments.

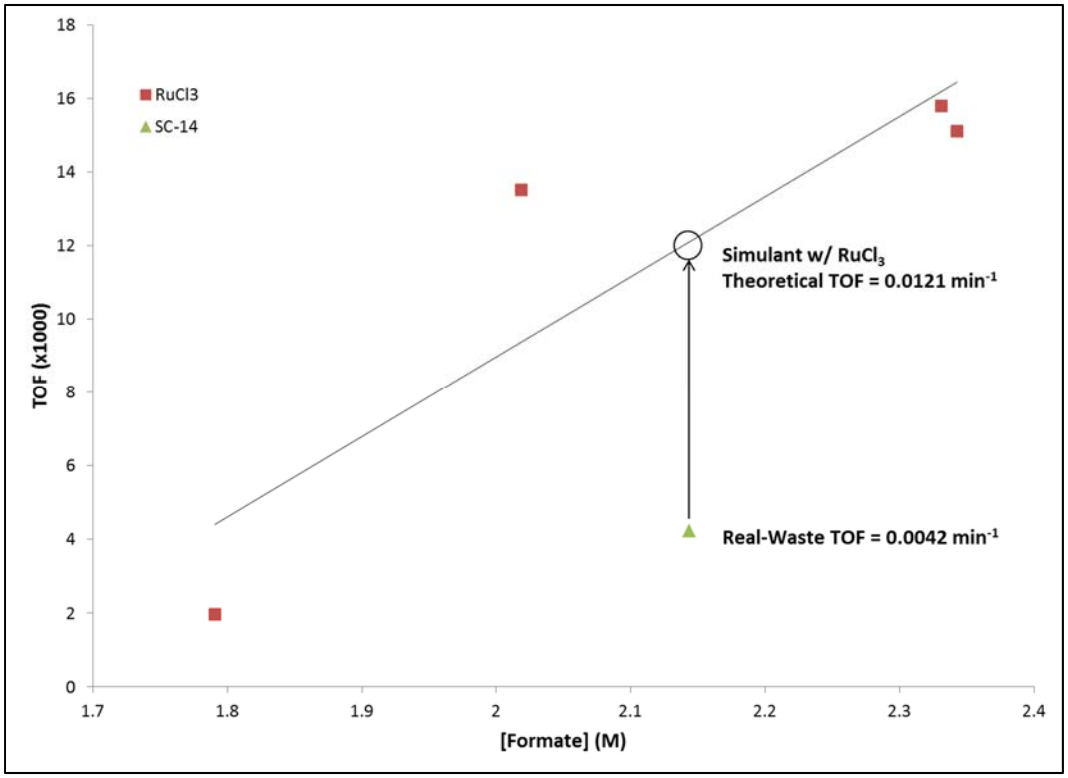

Figure 3-1. TOF of SB8 Testing Runs vs. Initial Formate Concentration. Black line represents linear trend in $RuCl_3$-containing simulant tests.

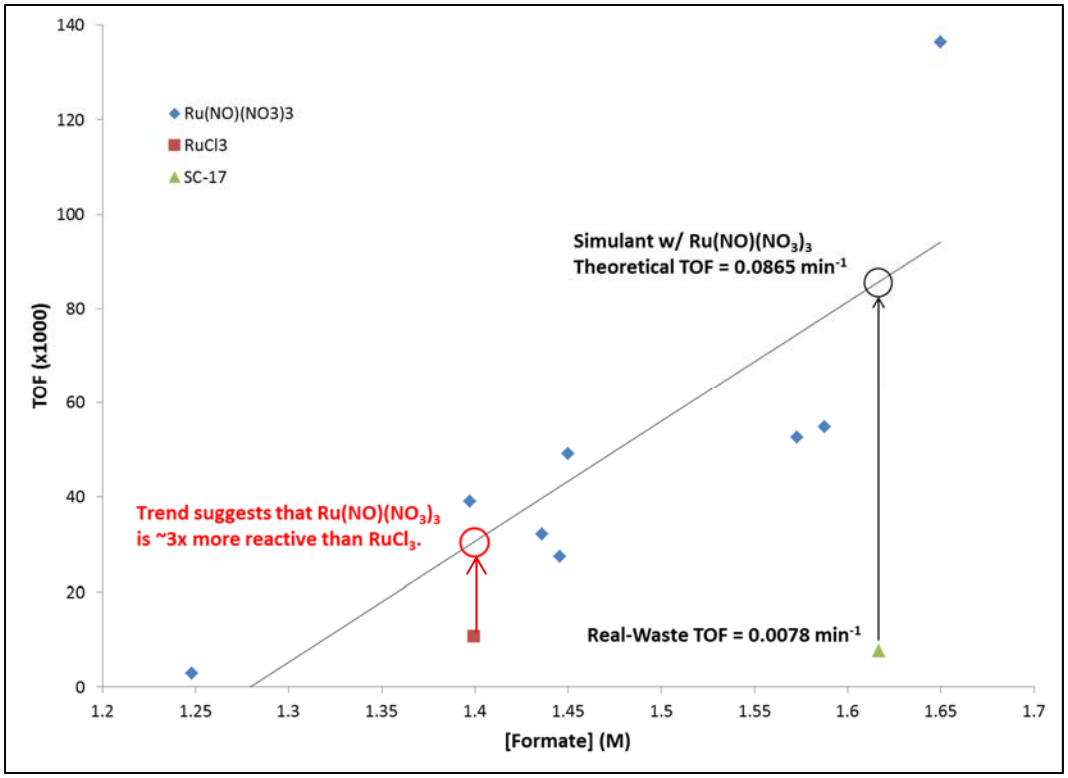

Figure 3-2. TOF of SB9 Testing Runs vs. Initial Formate Concentration. Black line represents linear trend in $Ru(NO)(NO_3)_3$-containing simulant tests. Red circle represents expected $RuCl_3$-containing system H_2 generation based on $Ru(NO)(NO_3)_3$-containing simulant trend.

The data shown in Figure 3-1 suggest that the catalysts present in $RuCl_3$-containing systems were approximately 3 (0.0121 min^{-1}/0.0042 min^{-1} = 2.9) times more active than the catalysts present in real-waste systems during the course of SB8 testing. Similarly, the data shown in Figure 3-2 suggest that the catalysts present in $Ru(NO)(NO_3)_3$-containing systems were approximately 11 (0.0865 min^{-1}/0.0078 min^{-1} = 11.1) times more active than the catalysts present in real-waste systems during the course of SB9 testing. The data for run SB9-A11 (shown in Figure 3-2) suggest that $Ru(NO)(NO_3)_3$-containing systems were approximately 3 (0.0303 min^{-1}/0.0108 min^{-1} = 2.8) times more reactive than $RuCl_3$-containing systems during SB9 testing.

Similar comparisons can be made with comparisons of TON to initial formate concentrations. Figure 3-3 gives the calculated TON of SB8 testing experiments (real-waste and simulant) plotted against estimated initial formate concentrations, while Figure 3-4 gives the calculated TON of SB9 testing (real-waste and simulant) experiments plotted against estimated initial formate concentrations.

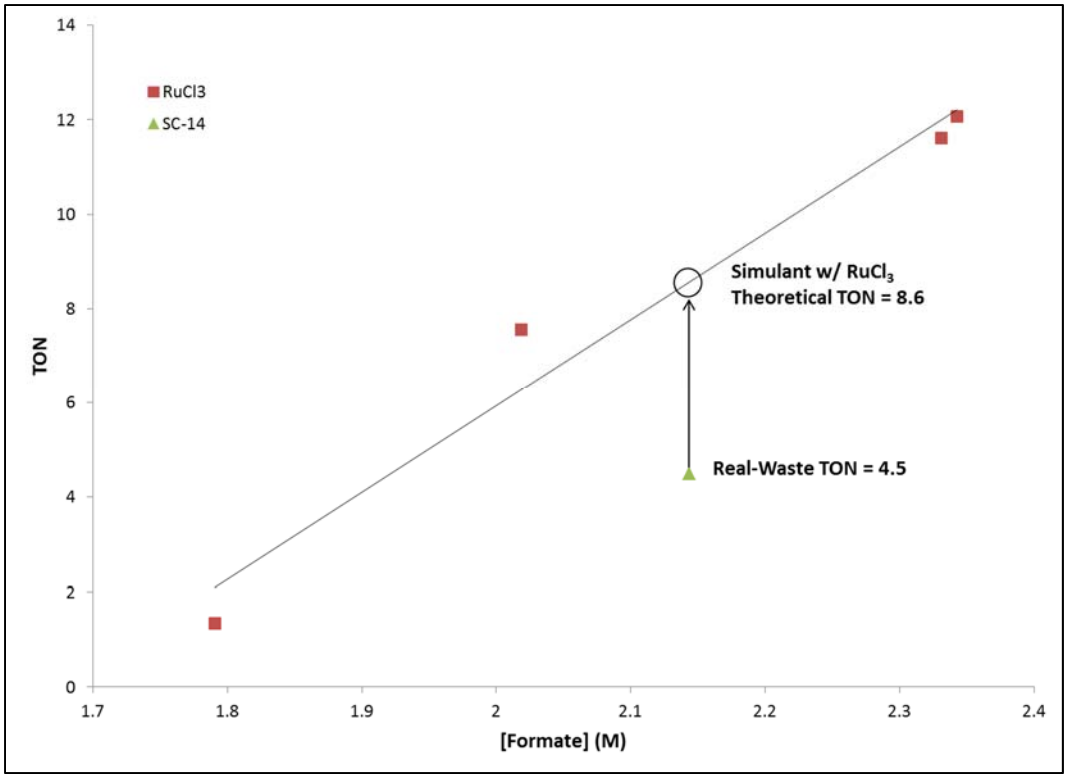

Figure 3-3. TON of SB8 Testing Runs vs. Initial Formate Concentration. Black line represents linear trend in simulant tests.

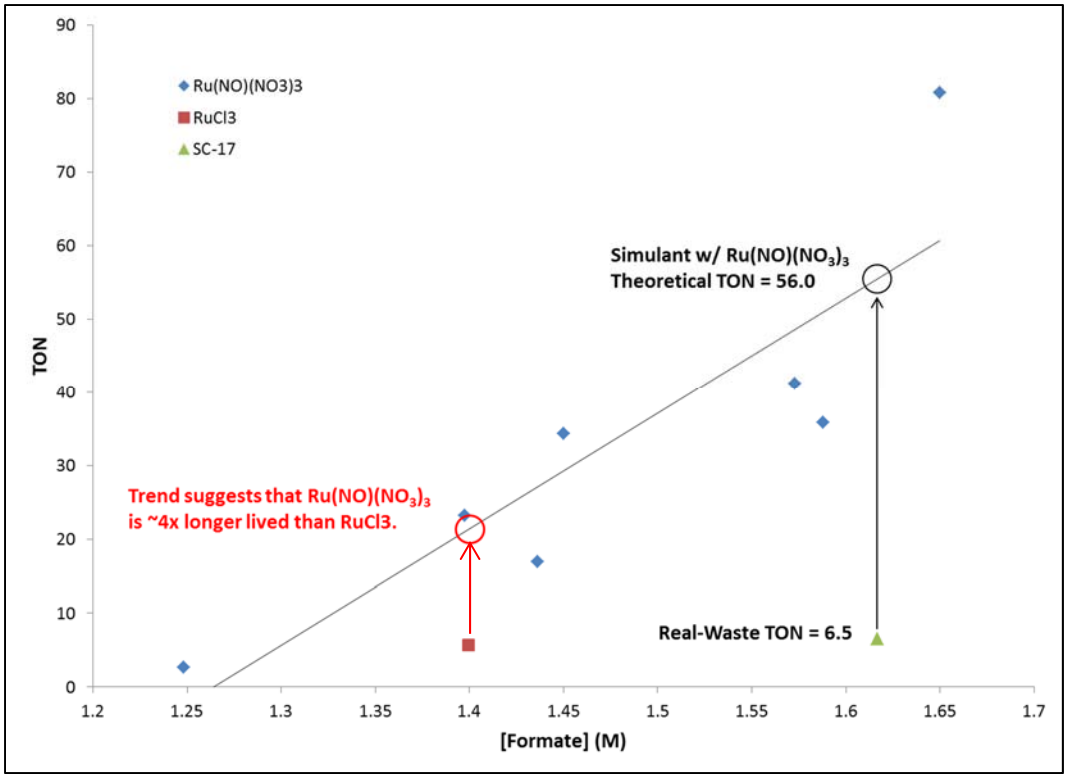

Figure 3-4. TON of SB9 Testing Runs vs. Initial Formate Concentration. Black line represents linear trend in simulant tests. Red circle represents expected real-waste generation based on simulant trend.

The data in Figure 3-3 suggest that the catalyst in $RuCl_3$-containing systems was approximately 2 (8.6/4.5 = 1.9) times more productive (underwent twice as many catalytic cycles, on average) than the catalyst present in real waste throughout SB8 testing. Likewise, the data in Figure 3-4 suggest that the catalyst in $Ru(NO)(NO_3)_3$-containing systems was approximately 9 (56.0/6.5 = 8.6) times more productive than the catalyst present in real waste throughout SB9 testing. Comparison of the measured TON for run SB9-11A ($RuCl_3$ run, shown in Figure 3-4) to the expected TON calculated from the trend seen in $Ru(NO)(NO_3)_3$ runs suggest that the catalyst involved in the systems containing the latter ruthenium source are approximately 4 (21.4/5.7 = 3.8) times more productive than systems containing the former ruthenium source. It is useful to note that run SB9-A7 was excluded from this analysis due to offgas measurement complications.

Results from these analyses suggest that both ruthenium sources are conservative with respect to hydrogen generation in terms of catalyst activity and productivity. $Ru(NO)(NO_3)_3$-containing systems appear to produce 9 times as much H_2 as real-waste systems at a rate that is approximately 11 times faster during maximum H_2 generation. $RuCl_3$-containing systems appear to produce 2 times as much H_2 as real-waste systems at a rate that is approximately 3 times faster during maximum H_2 generation. These results suggest that $RuCl_3$-containing systems are better simulants for real-waste H_2 generation. These results also indicate that the 125% addition of noble metals to sludge simulants is sufficiently conservative to bound real-waste behavior using either ruthenium source, and further suggest that noble metal additions as low as 100% might be employed conservatively in the case of sludge batch 8 and 9 processing.

3.2 Effects of Ruthenium Source Selection on N_2O Generation

Table 3-2 gives the TOFs and TONs for N_2O production during SB8 and SB9 simulant and real-waste testing. TOFs and TONs for N_2O are calculated analogously to the method described above for H_2.

Table 3-2. Catalytic Turnover Measurements for N_2O Production During SB8 and SB9 Flowsheet Testing Runs

Run ID	KMA (%)	Scale (L)	Form of Ru	TON	TOF (min^{-1})
SC-17 (SB9)	120	1	---	33.7	0.336
SB9-A2	105	4	$Ru(NO)(NO_3)_3$	17.4	0.181
SB9-A6	119	4	$Ru(NO)(NO_3)_3$	19.5	0.206
SB9-A11	119	4	$RuCl_3$	10.0	0.066
SB9-A8	123	1	$Ru(NO)(NO_3)_3$	38.7	0.158
SB9-A5	124	4	$Ru(NO)(NO_3)_3$	18.6	0.184
SB9-A7	124	1	$Ru(NO)(NO_3)_3$	38.9	0.176
SB9-A3	128	4	$Ru(NO)(NO_3)_3$	23.8	0.228
SB9-A4	129	1	$Ru(NO)(NO_3)_3$	41.2	0.298
SB9-A1	144	4	$Ru(NO)(NO_3)_3$	25.4	0.232
SC-14 (SB8)	109	1	---	88.0	0.496
SB8-D1	101	4	$RuCl_3$	5.9	0.035
SB8-D3	116	4	$RuCl_3$	5.9	0.019
SB8-D2	135	4	$RuCl_3$	3.5	0.021
SB8-D4	135	4	$RuCl_3$	8.5	0.031

It is obvious that systems containing $Ru(NO)(NO_3)_3$ produce larger amounts of N_2O at higher rates per mole of Ru present than systems containing $RuCl_3$, with $Ru(NO)(NO_3)_3$ runs yielding TONs between 17.4 and 41.2 and TOFs between 0.158 min^{-1} and 0.298 min^{-1}, relative to the TONs of 3.5-10.0 and TOFs of 0.0189-0.0659 min^{-1} seen in testing with $RuCl_3$-containing systems. It is important to note that during SB8 testing, simulant runs significantly underpredicted the production of N_2O, falling significantly short of both the TON and TOF achieved by SC-14 (88.0 and 0.496 min^{-1}, respectively). SB9 real-waste testing yielded similar results, with run SC-17 exhibiting a TOF of 0.336 min^{-1}. However, unlike SB8 testing, the $Ru(NO)(NO_3)_3$ runs employed in SB9 simulant testing sufficiently bound the SC-17 TON of 33.7. These results suggest that neither catalyst system perfectly reproduces N_2O production behavior seen in real-waste testing, although $Ru(NO)(NO_3)_3$-containing systems appear to be a better approximation.

It is important to note two observations concerning the conclusions drawn from N_2O production results. First, the catalytic production of N_2O in simulated nuclear waste is not as well understood as the catalytic production of H_2. Unlike H_2, only a portion of N_2O production is believed to be from catalyzed reactions. Likewise, mechanistic pathways for catalytic H_2 generation have been developed and explored[14], whereas no such research has been performed for N_2O. While previous reports have suggested an impact of Ru solubility on N_2O generation[3], it is unclear how significant this impact is when comparing experiments performed using sludges of significantly different composition. Second, the TONs calculated for SB9 tests (shown in Table 3-2) suggest that scale of the reaction may have a significant effect on production of N_2O. TONs for SB9-A 1-liter runs (SB9-A4, SB9-A7, and SB9-A8) are significantly higher than those seen in 4-liter runs (41.2, 38.9, and 38.7 compared to 25.4, 17.4, 23.8, 18.6, and 19.5). The reason for this apparent correlation is unknown, and it is recommended that future investigation be conducted on this correlation.

3.3 Effects of Ruthenium Source Selection on Anion Conversion

Table 3-3 gives the results of anion conversion reactions during SB8 and SB9 sludge simulant SRAT runs. The amount of destroyed formate is reported as the percentage of formate anion unaccounted for in the SRAT product relative to what was charged to the vessel as formic acid (i.e., presumed to be consumed by

reaction). The amount of nitrite converted into nitrate is reported as the change in slurry nitrate content relative to the amount of nitrite initially present in the slurry (also represented as a percent). Note that this number is often reported as a negative value, indicating consumption of nitrate by additional reactions (e.g., production of ammonia). The percentage of formate destruction attributable to H_2 formation is reported as the amount of H_2 produced relative to amount of formate destroyed during reaction.

Table 3-3. Anion Conversion Data for SB8 and SB9 Simulant and Real-Waste Testing

Run ID	Form of Ru	KMA (%)	NO_2^--to-N_2O Conversion (%)	NO_2^--to-NO_3^- Conversion (%)	Formate Destruction (%)	Formate Destruction Attributable to H_2 Formation (%)
SC-17 (SB9)	---	120	23.6	33	11	0.5
SB9-A2	$Ru(NO)(NO_3)_3$	105	19.6	14.4	35	0.3
SB9-A6	$Ru(NO)(NO_3)_3$	119	22.0	5.8	37	2.4
SB9-A11	$RuCl_3$	119	10.7	5.3	32	0.6
SB9-A8	$Ru(NO)(NO_3)_3$	123	43.7	-14	52	1.7
SB9-A5	$Ru(NO)(NO_3)_3$	124	21.0	5.3	44	3.4
SB9-A7	$Ru(NO)(NO_3)_3$	124	43.8	-7.9	44	0.3[a]
SB9-A3	$Ru(NO)(NO_3)_3$	128	26.9	-7.7	38	3.8
SB9-A4	$Ru(NO)(NO_3)_3$	129	46.6	4.6	40	3.2
SB9-A1	$Ru(NO)(NO_3)_3$	144	28.6	-20.1	52	7.1
SC-14 (SB9)	---	109	40.9	44	31	0.2
SB8-D1	$RuCl_3$	101	6.2	26	22	0.2
SB8-D3	$RuCl_3$	116	6.2	9	34	0.8
SB8-D2	$RuCl_3$	135	3.7	2	37	1.1
SB8-D4	$RuCl_3$	135	8.9	5	33	1.1

[a]Processing difficulties during run SB9-A7 caused issues with offgas measurement during the SRAT cycle, yielding unreliable estimates of total H_2 production.

In general, runs with ruthenium nitrosyl nitrate appear to consume more formate than real-waste experiments, with runs SB9-A1 through A8 yielding a range of formate destruction values of 35-52% (average of 43%) compared to the 11% formate destruction seen in SC-17. Additionally, these simulant runs appear to generate higher formate destruction values than those seen in SB8 testing, with runs SB8-D1 through D4 yielding formate destruction values between 22% and 37% (average of 32%). SB8 simulant runs appear to sufficiently mimic the behavior of real-waste in terms of formate destruction, with SC-14 yielding a formate destruction of 31%. A fraction of the difference between formate destruction values of $Ru(NO)(NO_3)_3$-containing systems and $RuCl_3$-containing systems may be explained by the increased hydrogen production (previously discussed).

Nitrite-to-nitrate conversion for SB9 $Ru(NO)(NO_3)_3$-containing systems vary widely, ranging from -20% to 14% (average of -2%), greatly underestimating the nitrite-to-nitrate conversion seen in real-waste testing (33% measured in SC-17). Similarly, nitrite destruction values for SB8 $RuCl_3$-containing systems underestimate the conversions seen in real-waste testing, with runs SB8-D1 through D4 yielding values of 2-26% (average of 10%) and SC-14 yielding a conversion of 44%. The simulant systems (SB8-D and SB9-A) appear to underestimate their respective real-waste systems to the same extent (34-35%), suggesting that choice of catalyst source has no appreciable impact on nitrite-to-nitrate conversion. This may be confirmed by comparing runs SC-17 (real waste, 120% KMA), SB9A-6 ($Ru(NO)(NO_3)_3$, 119% KMA), and SB9A-11 ($RuCl_3$, 119% KMA), which achieved nitrite-to-nitrate conversions of 33%, 5.8%, and 5.3%, respectively.

Plots of anion conversions versus KMA acid stoichiometry for SB9[3], SB8[6,9], SB7b[15], and SB7[16] testing are shown in Figure 3-5 (formate destruction) and Figure 3-6 (nitrite-to-nitrate conversion) for further comparison.

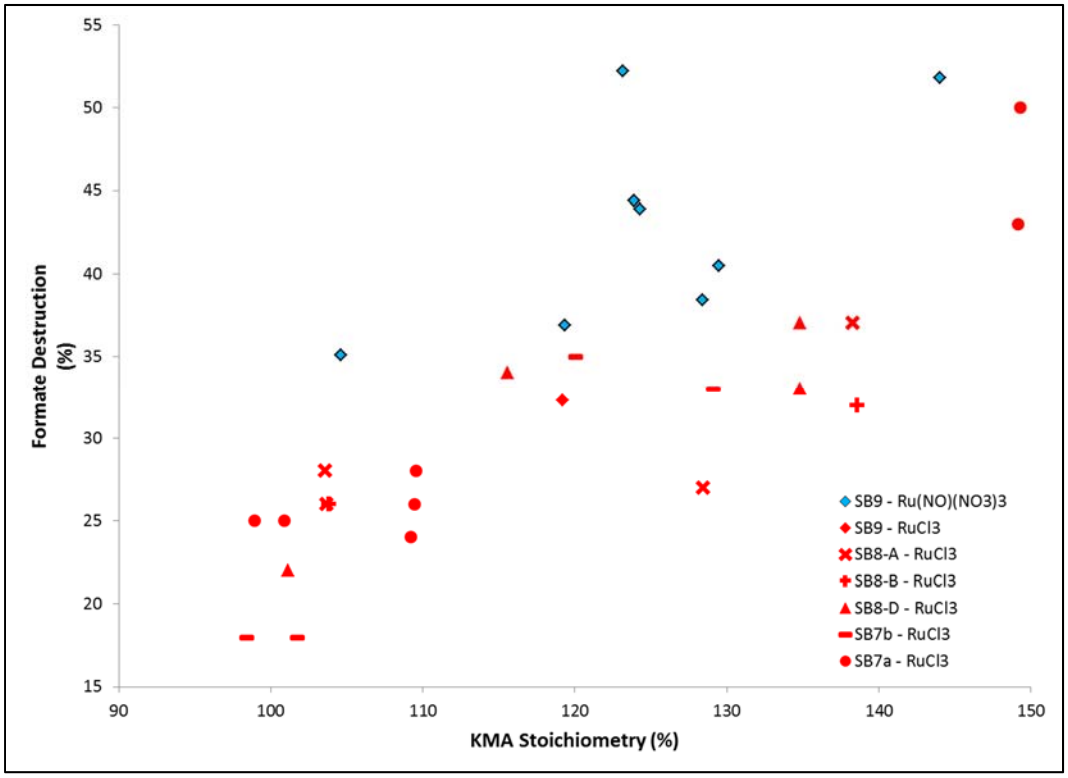

Figure 3-5. Formate Destruction (%) vs. KMA Stoichiometry (%) for SB9, SB8, SB7b, and SB7a Simulant Testing

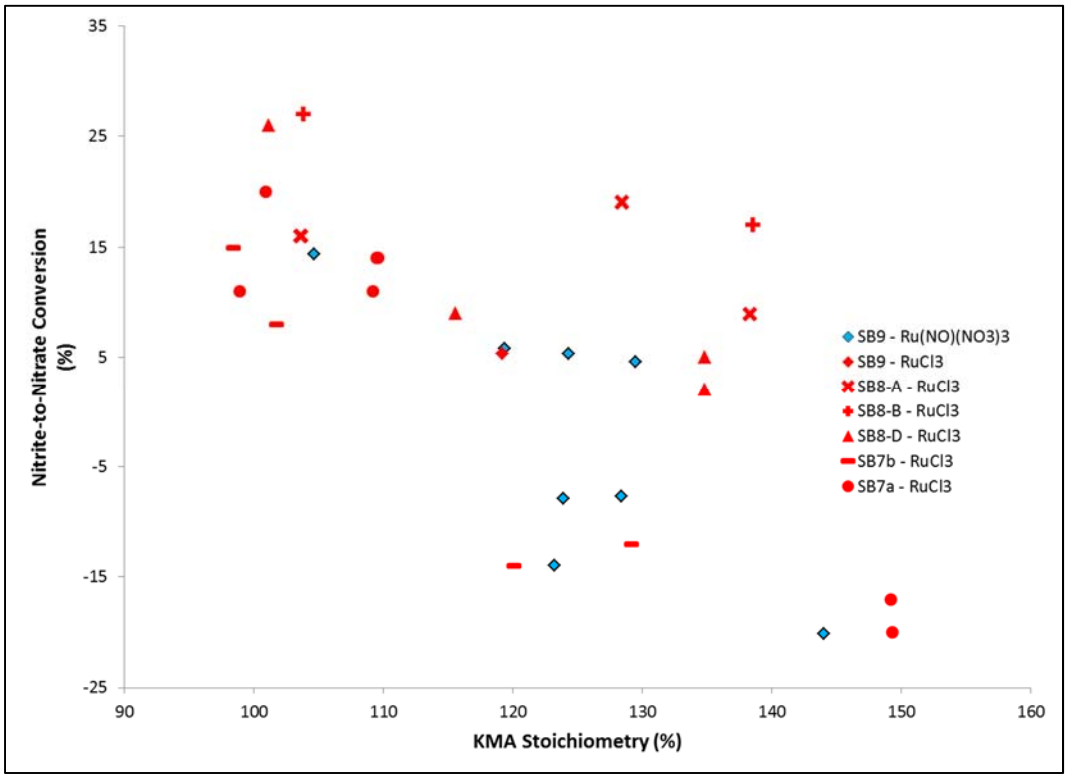

Figure 3-6. Nitrite-to-Nitrate Conversion (%) vs. KMA Stoichiometry (%) for SB9, SB8, SB7b, and SB7a Simulant Testing

Formate destruction data shown in Figure 3-5 shows patterns of clustering according to ruthenium source ("Blue" for $Ru(NO)(NO_3)_3$, "Red" for $RuCl_3$), which is consistent with the earlier observation that $Ru(NO)(NO_3)_3$-containing systems appear to consume more formate than $RuCl_3$-containing systems. However, less evidence of clustering is observed in the nitrite-to-nitrate conversion data shown in Figure 3-6, suggesting again that nitrite-to-nitrate conversion chemistry may not be dependent on ruthenium source selection.

Results from these analyses suggest that $RuCl_3$-containing systems are better simulants for predicting formate-destruction behavior. However, neither $RuCl_3$-containing systems nor $Ru(NO)(NO_3)_3$-containing systems predicted nitrite-to-nitrate conversions well during SB8 and SB9 testing. Rather, both catalyst systems appeared to underpredict nitrite-to-nitrate conversion to a similar extent. On this basis, it is suggested that $RuCl_3$-containing systems are better simulants for formate conversion.

3.4 Effects of Ruthenium Source Selection on Mercury Recovery and Removal

Table 3-4 gives the percentage of mercury recovered in the Mercury Water Wash Tank (MWWT) during SB8 and SB9 SRAT cycle simulations, relative to the amount of Hg initially charged to the vessel. Note that mercury and ruthenium were charged to simulant runs as a separate trim additions as HgO and $RuCl_3$ (SB8, Hg:Ru = 6.5-11.1:1) or HgO and $Ru(NO)(NO_3)_3$ (SB9, Hg:Ru = 16.4:1).

Table 3-4. Mercury Removal And Recovery Data for SB8 and SB9 Simulant Runs

Run ID	Form of Ru	KMA (%)	Hg Recovered in MWWT (%)
SB9-A2	$Ru(NO)(NO_3)_3$	105	9
SB9-A6	$Ru(NO)(NO_3)_3$	119	17
SB9-A11	$RuCl_3$	119	22
SB9-A8	$Ru(NO)(NO_3)_3$	123	34
SB9-A5	$Ru(NO)(NO_3)_3$	124	17
SB9-A7	$Ru(NO)(NO_3)_3$	124	12
SB9-A3	$Ru(NO)(NO_3)_3$	128	36
SB9-A4	$Ru(NO)(NO_3)_3$	129	25
SB9-A1	$Ru(NO)(NO_3)_3$	144	18
SB8-D1	$RuCl_3$	101	27
SB8-D3	$RuCl_3$	116	21
SB8-D2	$RuCl_3$	135	21
SB8-D4	$RuCl_3$	135	28

The data shown in Table 3-4 show that average MWWT Hg recovery values for $Ru(NO)(NO_3)_3$-containing systems during SB9 testing ranged between 9% and 36%, with an average recovery of 21%. Similar recoveries were seen during SB8 and SB9 testing with $RuCl_3$-containing systems, which ranged from 21% to 28% with an average recovery of 24%. From this data, it seems that recovery of mercury in the MWWT is not significantly affected by selection of ruthenium source.

These results suggest that selection of ruthenium source has no appreciable impact on mercury behavior in SRAT cycle processing. However, it is important to note that this lack of apparent correlation does not indicate the lack of Hg_2Cl_2 formation. During SB9-A11 (SB9 testing with $RuCl_3$), 0.814 g of $RuCl_3$ were trimmed into the sludge simulant along with 14.662 g of HgO. These masses correspond to 3.92 mmols of $RuCl_3$ (or 11.76 mmols of Cl^-) and 67.69 mmols of Hg. At this loading, ~17% (11.76/67.69 = 0.1737) of the mercury present could be transformed into Hg_2Cl_2. This value is less than the 20% uncertainty typically associated with Hg measurements. Given this observation, a single conclusion can be made: Poor mercury mass balance closure and large uncertainty on mercury measurements make it difficult to assess the full impact of chloride added as $RuCl_3$ on mercury behavior. This difficulty is exaggerated in sludge experiments with high Hg:Ru ratios (defined here as sludges with a mass ratio of Hg:Ru greater than 30:1, corresponding to the amount of $RuCl_3$ required to theoretically consume 20% of available Hg as Hg_2Cl_2) due to the inability of such sludges to form significant amounts of Hg_2Cl_2.

3.5 Effects of Ruthenium Source Selection Under the Nitric-Glycolic Flowsheet

Table 3-5 gives relevant results from each of the nitric-glycolic acid runs described in Section 2.3. Specifically, results for glycolate destruction, conversion to formate, conversion to oxalate, nitrite-to-nitrate conversion, and N_2O production (total and maximum rate) are shown for each run. Note that no data on H_2 production is given. This is because H_2 production under the nitric-glycolic flowsheet is negligible.

Table 3-5. Selected Results from Nitric-Glycolic Flowsheet Testing

Run ID	Ru Source	KMA (%)	Glycolate Destruction (%)	Conversion to Formate (%)	Conversion to Oxalate (%)	NO_2^- to NO_3^- (%)	N_2O Produced (mmol)	Max N_2O Rate (mmol/min)
SC-18	---	78	25.4	4.7	3.5	15.5	14.4	0.086
GN-70	Cl	102	18.7	2.3	1.5	30.9	26.5	0.111
GN-72	Cl	102	17.0	2.0	0.3	41.3	15.7	0.045
GN-74	Cl	102	14.5	1.6	0.0	35.6	19.6	0.059
GN-73	Cl	112	13.2	1.2	0.0	58.7	8.5	0.069
GN-75	Cl	112	15.3	1.3	0.7	55.0	20.7	0.180
GN-71	Cl	127	11.5	1.5	0.2	70.5	30.8	0.345
NG-58	NO_3	80	26.5	3.5	11.1	47.0	12.0	0.061
NG-51	NO_3	87	21.3	2.4	9.2	42.3	5.6	0.036
NG-53	NO_3	87	18.2	4.0	8.1	42.2	8.9	0.040
NG-55	NO_3	104	12.3	0.8	5.5	49.6	4.9	0.053
NG-55A	NO_3	104	14.0	1.2	5.9	62.2	4.7	0.055
NG-56	NO_3	104	13.5	0.9	7.4	66.0	2.9	0.033
NG-57	NO_3	104	13.8	0.7	5.9	51.5	4.7	0.057
NG-52	NO_3	121	12.8	1.5	3.4	66.7	15.3	0.148
NG-54	NO_3	121	9.0	0.9	2.3	73.6	8.8	0.061
NG-59	NO_3	128	10.4	1.9	3.1	72.0	4.9	0.068
NG-63	NO_3	110	NM	NM	NM	NM	25.9	0.361
NG-64	Cl	110	NM	NM	NM	NM	6.1	0.065

No trends are evident in the maximum generation rates of N_2O during the nitric-glycolic flowsheet simulations described above. Maximum N_2O generation rates for $Ru(NO)(NO_3)_3$-containing systems range from 0.033 (NG-56) to 0.361 (NG-63) mmol/min, while rates for $RuCl_3$-containing systems range from 0.045 (GN-72) to 0.345 (GN-71) mmol/min. Both of these ranges bound the maximum generation rate seen in SC-18 (0.086 mmol/min). It is important to note, however, that SC-18 was performed at 78% KMA, placing it far outside of the stoichiometric range explored by the scaled testing (GN70-75), thereby allowing no direct comparison between $RuCl_3$-containing simulant systems and real-waste systems. Similarly, no trend can be seen concerning the total production of N_2O. $Ru(NO)(NO_3)_3$-containing systems exhibited N_2O production between 2.9 (NG-56) and 25.9 (NG-63) mmol, while $RuCl_3$-containing systems produced between 6.1 (NG-64) and 30.8 (GN-71) mmol. Again, both of these ranges sufficiently bound the total production of N_2O from SC-18 (14.4 mmol).

Interestingly, trends can be seen in anion conversion data presented in Table 3-5. Figure 3-7 shows the destruction of glycolate (expressed as a percentage of glycolate charged to the vessel) exhibited by the $Ru(NO)(NO_3)_3$-containing NG-series experiments, the $RuCl_3$-containing GN-series experiments, and SC-18 as a function of acid stoichiometry.

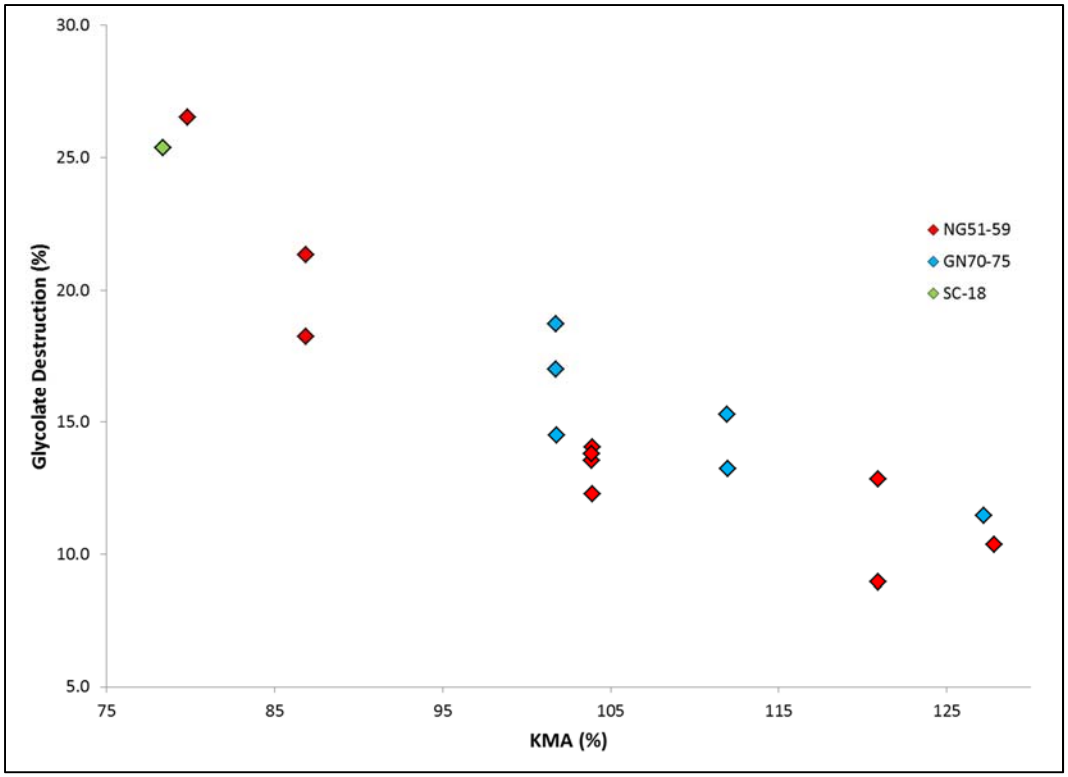

Figure 3-7. Glycolate Destruction as a Function of Acid Stoichiometry for Nitric-Glycolic Flowsheet Simulations

Upon inspection of Figure 3-7, a few observations may be made: 1.) the percentage of glycolate destruction appears to trend downward with increasing acid stoichiometry, 2.) results from $Ru(NO)(NO_3)_3$-containing experiments are more or less indistinguishable from those of $RuCl_3$-containing experiments, and 3.) glycolate destruction from SC-18 seems to fall neatly in line with results from NG-series runs and GN-series runs. These three observations suggest that glycolate destruction is not dependent on ruthenium source selection. A similar conclusion can be made for conversion to formate data, shown in Figure 3-8. These observations and conclusions have been noted previously in a report detailing the statistical evaluation of chemical reactions under the nitric-glycolic flowsheet.[17]

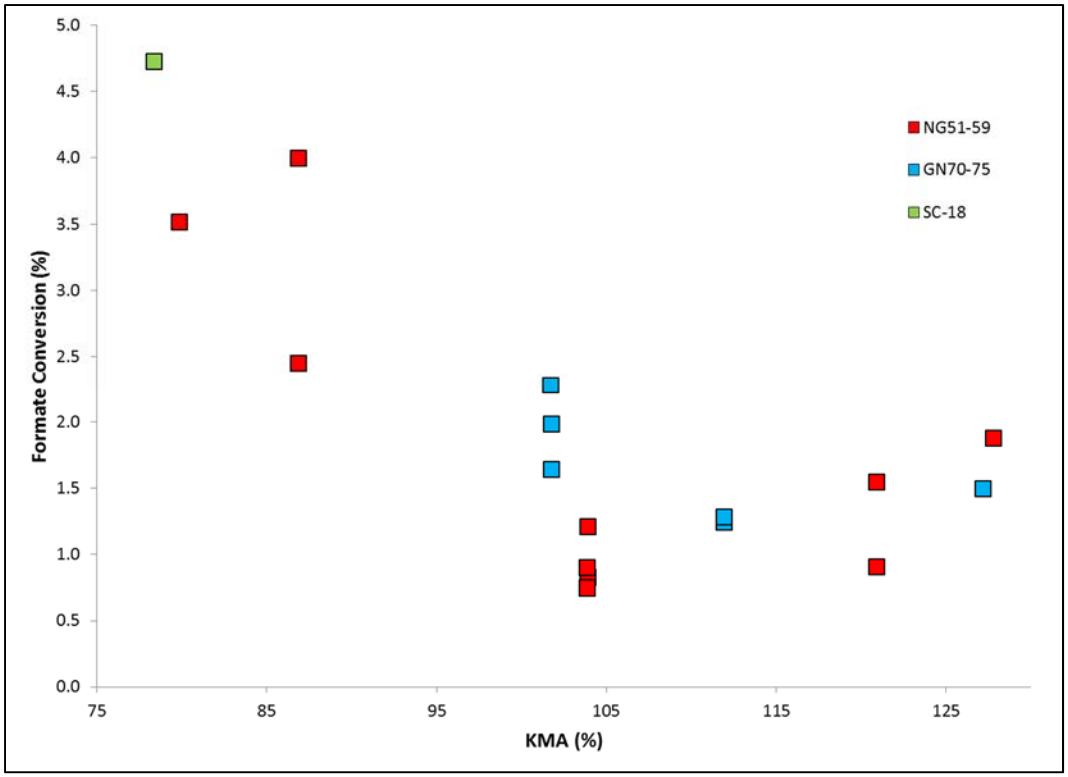

Figure 3-8. Conversion to Formate as a Function of Acid Stoichiometry for Nitric-Glycolic Flowsheet Simulations

Again, for the data in Figure 3-8, it seems that 1.) both $Ru(NO)(NO_3)_3$-containing systems and $RuCl_3$-containing systems exhibit similar formate conversion behavior as a function of acid stoichiometry (large negative slopes at stoichiometries less than 105%, slightly positive slopes at stoichiometries greater than 105%), and 2.) formate conversion from SC-18 appears to fall in the same trendline suggested by simulant data. These results suggest that ruthenium source selection has no major effect on conversion of glycolate to formate.

Figure 3-9 shows the conversions of nitrite to nitrate (expressed as a percentage of nitrite charged) exhibited by the nitric-glycolic experiments described above.

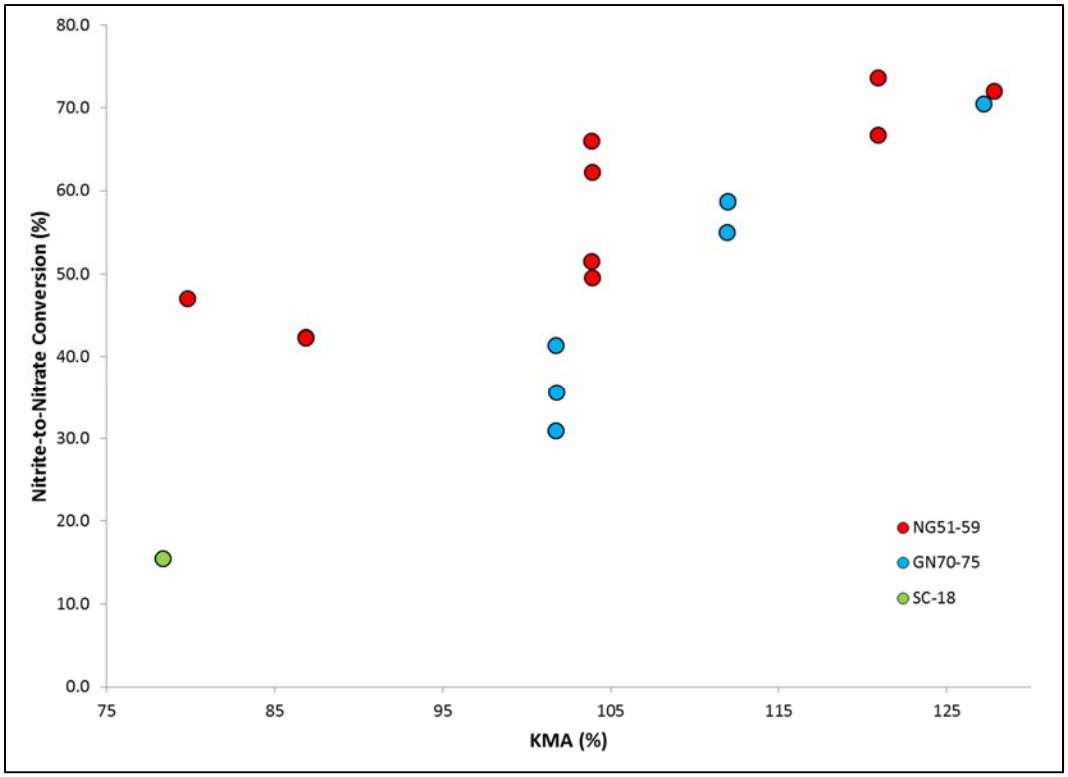

Figure 3-9. Nitrite-to-Nitrate Conversion as a Function of Acid Stoichiometry for Nitric-Glycolic Flowsheet Simulations

From the data shown in Figure 3-9, it is not evident that real waste experiments (SC-18) behave similarly to either $Ru(NO)(NO_3)_3$-containing systems or to $RuCl_3$-containing systems. NG-series runs appear to overpredict the nitrite-to-nitrate conversion, with NG-58 yielding a value of 47% at an acid stoichiometry of 80% (relative to the value of 15.5% nitrite-to-nitrate conversion experienced by SC-18 at a stoichiometry of 78%). While the $RuCl_3$-containing GN-series runs appear to trend with lower conversions (31% experienced by GN-70 at an acid stoichiometry of 102%), it is unclear if these systems could sufficiently reproduce the behavior seen in SC-18 at a stoichiometry of 78%. The data appears inconclusive, and more work is recommended to further investigate the behavior of nitrite-to-nitrate conversion in the glycolic acid flowsheet.

Oxalate conversions (expressed as a percentage of charged glycolate) are given in Figure 3-10.

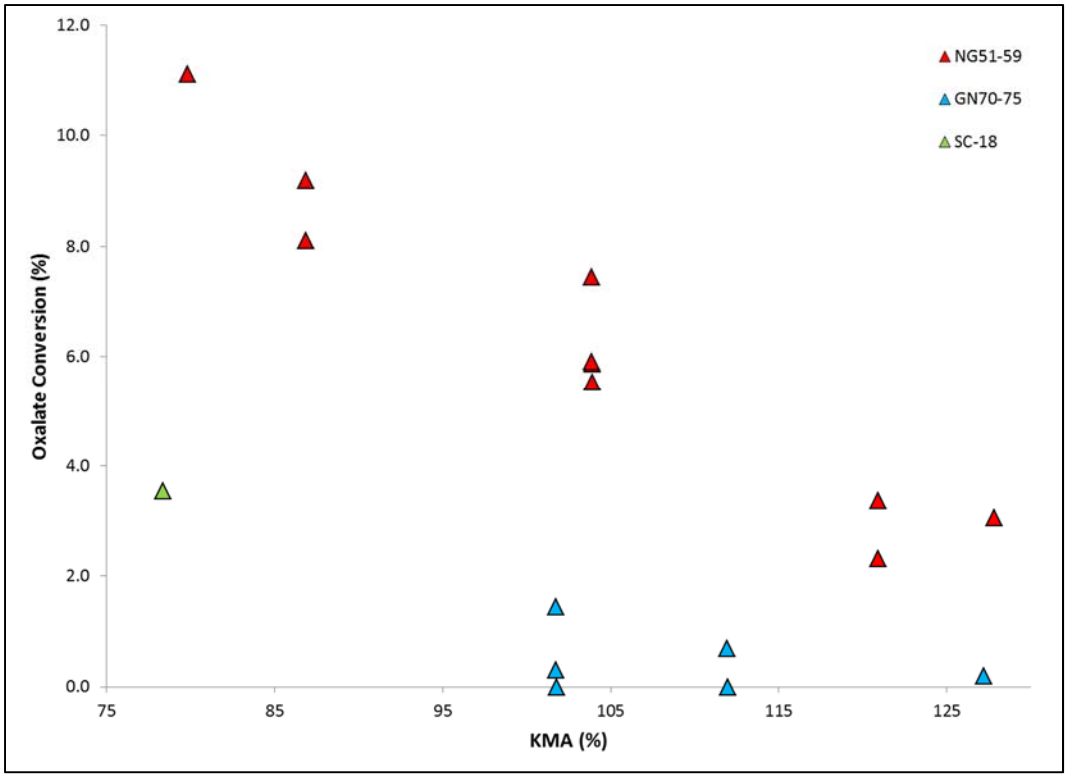

Figure 3-10. Oxalate Conversion as a Function of Acid Stoichiometry for Nitric-Glycolic Flowsheet Simulations

From the data in Figure 3-10, a number of observations can be made. First, it is apparent that $Ru(NO)(NO_3)_3$-containing systems follow a trend of decreasing oxalate conversions with increasing acid stoichiometry (it is unclear if any such trend is present in the data from $RuCl_3$-containing systems). Second, it is apparent that the trend exhibited by the NG-series experiments significantly overpredicts the oxalate conversion seen in SC-18. Finally, the oxalate conversions exhibited in $Ru(NO)(NO_3)_3$-containing systems appear to significantly exceed those of $RuCl_3$-containing systems, which matches the observations made by Zamecnik after performing a series of statistical analyses on the results of several nitric-glycolic flowsheet simulations.[17] It is important to note that Zamecnik observed several differences in these sludge batches capable of explaining the variation in oxalate production, so it must not be assumed that ruthenium form is conclusively the most important factor. To date, insufficient real-waste testing has been performed under the nitric-glycolic flowsheet to sufficiently assess the ability of either catalytic system ($RuCl_3$ or $Ru(NO)(NO_3)_3$) to adequately describe or bound the glycolate-oxalate conversion behavior in real-waste. Additional real-waste and simulant testing is recommended to further investigate this relationship.

4.0 Conclusions

Based on the analyses described in this report, the following conclusions can be made:

Nitric-Formic Flowsheet

- Both $RuCl_3$- and $Ru(NO)(NO_3)_3$-containing systems appear to be conservative in terms of H_2 production with respect to real-waste values, with $Ru(NO)(NO_3)_3$-containing systems exhibiting significantly more conservatism than $RuCl_3$-containing systems.
- Neither catalytic simulant system is conservative in terms of N_2O production with respect to real-waste values. Of the two, $Ru(NO)(NO_3)_3$-containing systems appear to underpredict the least.

- Reaction scale appears to have an effect on N_2O production and may partially explain the tendency of 4-L simulant testing to underpredict N_2O production rates seen in 1-L real waste testing.
- $RuCl_3$-containing systems and $Ru(NO)(NO_3)_3$-containing systems behave differently in terms of formate destruction. This may be due to differences beyond those seen in H_2 production (such as oxidation of formate or H_2). $RuCl_3$-containing systems appear to better emulate the formate destruction seen in real waste testing.
- Nitrite-to-nitrate conversion does not appear to be significantly affected by selection of ruthenium source.
- Based on available data, ruthenium source does not appear to have any significant effect on mercury removal or recovery during SRAT processing.
- Poor mercury balance makes the affirmation of effects due to Hg_2Cl_2 formation difficult.
- Given the ratio of Ru to Hg used in SB9 testing, the presence of chloride from $RuCl_3$ added to simulant is not expected to affect the majority of mercury via formation of Hg_2Cl_2.

Nitric-Glycolic Flowsheet

- Glycolate destruction and conversion to formate do not appear to be significantly affected by the selection of ruthenium source.
- $Ru(NO)(NO_3)_3$-containing systems tend to convert more of the initially-charged nitrite and glycolate to nitrate and oxalate (respectively) than $RuCl_3$-containing systems.
- Simulant experiments conducted with $Ru(NO)(NO_3)_3$ appear to overpredict the conversion of nitrite to nitrate. No conclusion can be drawn concerning this effect in $RuCl_3$-containing systems.
- Simulant experiments conducted with $Ru(NO)(NO_3)_3$ appear to overpredict the conversion of glycolate to oxalate. It is uncertain if $RuCl_3$-containing systems can adequately predict the conversion of glycolate to oxalate.

5.0 Recommendations

Based on the conclusions stated in Section 4.0, the following recommendations have been made:

1. In future SB testing under the nitric-formic flowsheet,

    - $RuCl_3$ should be used when it is more important to accurately emulate H_2 production behavior or formate destruction seen in real-waste. This will allow simulant runs to be performed conservatively, but not so much as to impractically bound any recommended acid stoichiometry window proposed during future flowsheet testing.
    - $Ru(NO)(NO_3)_3$ should be used when it is more important to accurately emulate N_2O production behavior seen in real waste, or when mercury behavior is being investigated in Low Hg/High Ru sludges (Hg:Ru mass ratio of 30:1 or lower). This will guarantee that minimal Hg_2Cl_2 will be formed during processing and more closely predict the formation of N_2O.
    - When the factors described above are negligible either ruthenium source may be used, with consideration given to availability and ease of use.

2. Further investigation should be made into the effect of scale on the production of N_2O and what effects that relationship has on the data presented in this report. In particular, effort should be made to determine the flowsheet dependence of this phenomenon and the applicability of comparison between 4-L simulant experiments to 1-L real-waste experiments.

3. Additional real-waste experiments should be performed under the nitric-glycolic flowsheet so that the chemical behavior of glycolic acid in real waste can be better defined. Since neither hydrogen production nor formate destruction are significant factors under the nitric-glycolic flowsheet, no recommendation can be made concerning the use of either ruthenium source in nitric-glycolic

flowsheet testing. Once additional real-waste testing data is available, a re-evaluation should be made concerning the effect of ruthenium source on conversion of glycolate to oxalate and nitrite to nitrate. If feasible, future simulant tests under the nitric-glycolic flowsheet should include duplicate runs using both sources of ruthenium in order to provide a better understanding of the importance of source selection on processing behavior.

6.0 References

1. D.C. Koopman, “Dwpf Hydrogen Generation Study-Form of Noble Metal Srat Testing,” Savannah River National Laboratory, Aiken, SC, WSRC-TR-2005-00286, 2005.
2. J.R. Zamecnik, Woodham, W.H., Williams, M.S., "*Dwpf Chemical Processing Cell (Cpc) Alternate Reductant Chemistry Testing - Proposed Work*," Savannah River National Laboratory, **SRNL-L3100-2016-00075**, 2016.
3. T.E. Smith, J.D. Newell, and W.H. Woodham, “Defense Waste Processing Facility Simulant Chemical Processing Cell Studies for Sludge Batch 9,” Savannah River National Laboratory, Aiken, SC, SRNL-STI-2016-00281, Rev 0, 2016.
4. A. Samadi-Dezfouli, "Sludge Batch 9b Simulant Flowsheet Studies," Savannah River Remediation, **U-TTR-S-00043**, 2017.
5. J.D. Newell, Woodham, W.H., "Task Technical and Quality Assurance Plan for the Recommendation of Ruthenium Catalyst for Sludge Batch Simulant Studies," Savannah River National Laboratory, **SRNL-RP-2017-00245**, 2017.
6. D.C. Koopman and J.R. Zamecnik, “Dwpf Simulant Cpc Studies for Sb8,” Savannah River National Laboratory, Aiken, SC, SRNL-STI-2013-00106, Rev. 0, 2013.
7. J.M. Pareizs and C.L. Crawford, “Sludge Washing and Demonstration of the Dwpf Flowsheet in the Srnl Shielded Cells for Sludge Batch 8 Qualification,” Savannah River National Lab, Aiken, SC, SRNL-STI--2013-00116, 2013.
8. J. Pareizs, D. Newell, C. Martino, C. Crawford, and F. Johnson, “Sludge Washing and Demonstration of the Dwpf Nitric/Formic Flowsheet in the Srnl Shielded Cells for Sludge Batch 9 Qualification,”; Savannah River Site (SRS), Aiken, SC (United States), SRNL--STI-2016-00355 United States 10.2172/1330956 available SRS English, 2016.
9. J.D. Newell, "Dwpf Simulant Cpc Studies for Sb8," Savannah River National Laboratory, **SRNL-STI-2012-00620**, 2012.
10. D.P. Lambert, J.R. Zamecnik, J.D. Newell, C.J. Martino, "Impact of Scaling on the Nitric-Glycolic Acid Flowsheet," Savannah River National Laboratory, **SRNL-STI-2014-00306**, 2016.
11. M.S.W. D.P. Lambert, C.H. Brandenburg, M.C. Luther, J.D. Newell, W.H. Woodham, “Srnl-Sti-2016-00319 *Sludge Batch 9 Simulant Runs Using the Nitric-Glycolic Acid Flowsheet*,” Savannah River National Laboratory, Aiken, SC, 2016.
12. D.P. Lambert, M.S. Williams, C.H. Brandenburg, "Antifoam Degradation Testing to Support Development of Sludge Batch 9 Flammability Strategy," Savannah River National Laboratory, **SRNL-L3100-2016-00146**, 2016.
13. J.D. Newell, J.M. Pareizs, C.J. Martino, S.H. Reboul, C.J. Coleman, T.B. Edwards, F.C. Johnson, "Actual Waste Demonstration of the Nitric-Glycolic Flowsheet for Sludge Batch 9 Qualification," Savannah River National Laboratory, **SRNL-STI-2016-00327, Rev 1**, 2017.
14. R.B. King, Bhattacharyya, N.K., “Catalytic Reactions of Formate Part 4. A Nitrite-Promoted Rhodium(Iii) Catalyst for Hydrogen Generation from Formic-Acid in Aqueous-Solution,” *Inorganica Chimica Acta*, **237** [1-2] 65-39 (1995).
15. D.C. Koopman, “Dwpf Simulant Cpc Studies for Sb7b,” Savannah River National Lab, Aiken, SC, SRNL-STI-2011-00547, Revision 0, 2011.
16. A.I. Fernandez and D.C. Koopman, “Sludge Batch 7 Qualification and Flowsheet Chemical Process Cell Simulations,” Savannah River National Lab, Aiken, SC, SRNL-STI-2011-00006, Revision 1, 2011.
17. J.R. Zamecnik, Edwards, T.B., "Defense Waste Processing Facility Nitric-Glycolic Flowsheet Chemical Process Cell Chemistry: Part 2," Savannah River National Laboratory, **SRNL-STI-2017-00172**, 2017.